Identification of Nonradiative Decay Pathways in Cy3

Citation: Hart, Stephanie M. et al. "Identification of Nonradiative Decay Pathways in Cy3." Journal of Physical Chemistry Letters 11, 13 (June 2020): 5000-5007. © 2020 American Chemical Society

As Published: http://dx.doi.org/10.1021/acs.jpclett.0c01201

Publisher: American Chemical Society (ACS)

Persistent URL: https://hdl.handle.net/1721.1/132933

Version: Author's final manuscript: final author's manuscript post peer review, without publisher's formatting or copy editing

Identification of Non-radiative Decay Pathways in Cy3

Stephanie M. Hart,[†] James L. Banal,[‡] Mark Bathe,[‡] and Gabriela S. Schlau-Cohen[*,†]

†*Department of Chemistry, Massachusetts Institute of Technology, Cambridge, MA 02139 USA*

‡*Department of Biological Engineering, Massachusetts Institute of Technology, Cambridge, MA 02139 USA*

E-mail: gssc@mit.edu

Abstract

Photoexcited fluorescent markers are extensively used in spectroscopy, imaging, and analysis of biological systems. The performance of fluorescent markers depends on high levels of emission, which are limited by competing non-radiative decay pathways. Small-molecule fluorescent dyes have been increasingly used as markers due to their high and stable emission. Despite their prevalence, the non-radiative decay pathways of these dyes have not been determined. Here, we investigate these pathways for a widely-used indocarbocyanine dye, Cy3, using transient grating spectroscopy. We identify a non-radiative decay pathway via a previously unknown dark state formed within $\sim$ 1 ps of photoexcitation. Our experiments, in combination with electronic structure calculations, suggest that the generation of the dark state is mediated by picosecond vibrational mode coupling, likely via a conical intersection. We further identify the vibrational modes, and thus structural elements, responsible for the formation and dynamics of the dark state, providing insight into suppressing non-radiative decay pathways in fluorescent markers such as Cy3.

Graphical TOC Entry

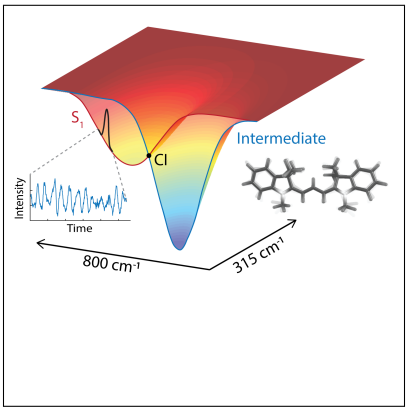

Keywords

ultrafast spectroscopy; Cy3; vibrational wavepackets

Small-molecule fluorophores are ubiquitous tools in microscopy, spectroscopy, and biological assays, providing multiscale resolution to understand systems from organisms to single-molecule scales with molecular specificity.[1–3] The diversity of chemical structures for polyaromatic organic flurophores has also been used in solar concentrators, light-emitting diodes, and lasers.[4–7] All of the applications of fluorophores rely on robust photophysical behaviour that is limited by dark state formation via isomerization, intersystem crossing to triplet states, and generation of radical species.[5,8–10] Optimizing the molecular structure of dyes can overcome these limitations by enhancing fluorophore photostability based on known structural dynamics associated with dark state formation.[2,11,12] However, the requisite knowledge of structural dynamics has been limited to longer timescale phenomena because, to date, there have been few investigations on the femtosecond timescale.[13,14] Therefore, the relevant structural dynamics for ultrafast dark state formation have not been identified, despite their potential for fluorophore optimization.

Ultrafast spectroscopy has characterized dynamics on the femtosecond timescale in a wide range of systems.[15–20] These experiments have provided critical insight into excited state photophysical processes such as electron transfer, potential energy surface crossing, and intersystem crossing.[18,21–25] Along with electronic processes alone, ultrafast spectroscopy can probe coupling between electronic processes and nuclear motion, including excited state reactivity and vibrationally-mediated energy transfer.[26,27] Despite the rich information that can be derived from such investigations, they have been minimally used to examine femtosecond to picosecond dynamics in certain types of widely-used small-molecule fluorophores.

Cyanines are a family of small-molecule fluorophores commonly used as fluorescent markers for biological imaging and detection assays because of their large absorption cross-sections and stable emission.[28–30] In recent years, cyanines have also been studied as a model photoisomerization system, and are one of few molecular classes that have successfully undergone coherent reactivity control schemes.[31,32] Cyanines consist of two nitrogen atoms connected by a conjugated polymethine bridge. In visible-range cyanines, photoinduced excitation to

the S_1 state proceeds through a π–π^* transition of the conjugated system, after which population relaxation occurs via a combination of radiative fluorescence, non-radiative internal conversion, photoisomerization to a dark state, and intersystem crossing.

Visible-range cyanines such as the indole-based Cy3, Cy5, and their derivatives are particularly widely used as fluorescent markers. In this cyanine sub-family, the major known non-radiative decay pathway occurs along the photoisomerization reaction coordinate. After photoexcitation from the trans ground state, isomerization to the cis configuration begins through picosecond to nanosecond generation of a twisted 90° angle configuration. The twisted configuration has an optically dark state with charge-transfer character (twisted intramolecular charge-transfer state or TICT), which relaxes back to the trans ground state or to the cis ground state.[33–35] Although ultrafast spectroscopy has been used extensively to characterize the barrierless photoisomerization of cyanines such as the quinoline-based pseudoisocyanine and pinacyanol,[36,37] cyanines such as Cy3 and Cy5 must overcome an energetic activation barrier to populate the TICT state. Therefore, the barrierless dynamics previously characterized cannot be extrapolated to other cyanines. Despite their wide usage, the femtosecond dynamics of the Cy3 and Cy5 sub-family have been minimally investigated. Specifically, the number and role of dark states and how nuclear motions govern the excited state pathways has not been determined.

Here, we investigate the femtosecond dynamics of Cy3 (Figure 1a, inset). Using homodyne transient grating spectroscopy, we monitor the excited state evolution of Cy3 including population relaxation and the generation of nuclear wavepackets. Time-domain frequency analysis of these wavepackets as a function of emission frequency identifies several long-lived vibrational modes along with coupling between modes that persists for $\sim$1.5 ps after photoexcitation. The phase of the wavepackets reveals a previously unknown non-emissive trans intermediate state that persists for several picoseconds after photoexcitation, providing an alternate non-radiative relaxation pathway. The existence and dynamics of the identified trans intermediate competes with radiative emission, and thus hinders performance as a bi-

ological marker. Observation of this state, and particularly the nuclear motion underlying its formation, provides a target for molecular engineering, and thus has the potential to establish design principles for fluorophore structure engineering for enhanced emission.

The linear absorption spectrum of Cy3 is shown in Figure 1a along with the emission spectrum. Both spectra exhibit a vibronic progression of the 0–0, 0–1, and 0–2 transitions with 1205 cm^{-1} spacing, corresponding to a C–C stretching mode,[38] and a Huang-Rhys factor of 0.53 (Supporting Information Figure 6a). While the emission spectrum retains signatures of a vibronic progression, the lack of mirror symmetry with the absorption spectrum likely arises from excited state structural reorganization of the polymethine backbone. The Stokes shift is 530 cm^{-1}, corresponding to a reorganization energy of 265 cm^{-1}.

Ultrafast, emission frequency-resolved transient grating measurements were performed with broadband pulses centered at $19,300$ cm^{-1} (Figure 1a, gray). Transient grating spectroscopy is a four-wave mixing technique performed in a non-collinear geometry for background free, and thus high sensitivity, detection. Here, we monitor excited state population and coherence dynamics. Figure 1b shows a representative time trace at an emission frequency of $\omega_3 = 18,620$ cm^{-1}. Short timescale population relaxation appears as a decay on two timescales, $\sim$70 fs and $\sim$4 ps. We assign both of these timescales to excited state vibrational relaxation (further details given in Section 4 of Supporting Information). Long-timescale population relaxation appears as a decay on a $\sim$45 ps timescale, likely due to conversion from the bight excited state to the TICT state (Supporting Information Figure 6).

Coherent vibrational wavepacket propagation appears as oscillatory features in the time domain traces. These oscillations correspond to wavepackets on the ground and excited state potential energy surfaces and persist for several picoseconds after photoexcitation, which have been observed in similar cyanine systems.[39,40] A Fourier transform along the time axis of the transient grating data (t_2) recovers the mode frequencies. The resultant power spectra are shown in Figure 1c for three emission frequencies ($18,620$ cm^{-1}, $18,050$ cm^{-1}, and $17,450$

cm^{-1}), which span the ground state bleach and stimulated emission peaks. The traces show several modes between 35 cm^{-1} and $1,594$ cm^{-1}. All of these are present in the non-resonant Raman spectrum (Figure 1c, bottom). A complete assignment of the modes present in the transient grating power spectra is shown in the Supporting Information Section 2, primarily based on density functional theory (DFT) calculations.

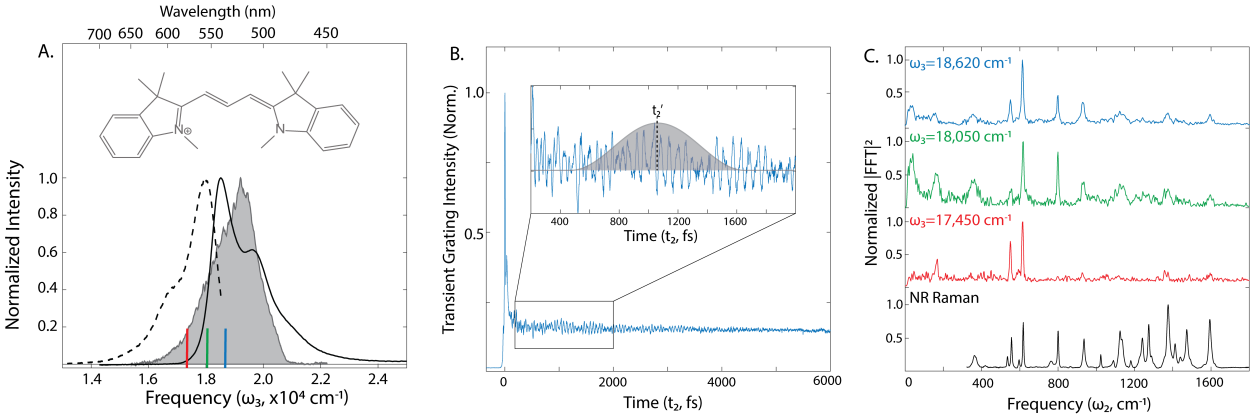

Figure 1: Cyanine dye vibronic dynamics. (A) Cyanine dye (commercially basic red 12, inset) absorption (solid) and emission (dashed) spectra showing a strong vibronic progression. Laser pulse is shown in gray. (B) Time domain transient grating trace from frequency-resolved homodyne detection for $\omega_3 = 18,620$ cm^{-1}. The window used in the sliding window Fourier transform analysis in Figure 2a is shown in gray. Here t_2' denotes the center time of the window. (C) Power spectra of decay-subtracted residuals at selected emission frequencies along with the non-resonant Raman spectrum.

The temporal evolution of the coherent oscillations observed in the transient grating signal were extracted using a sliding window Fourier transform. A 600 fs Hann window was used as the filtering function and is shown over the time domain trace in Figure 1b. We denote the time axis generated by the sliding Fourier window, t_2'. The resultant frequency-time plot (ω_2, t_2') is shown for $\omega_3 = 18,620$ cm^{-1} in Figure 2a. Several long-lived modes are observed at 550 cm^{-1}, 615 cm^{-1}, 800 cm^{-1}, and 928 cm^{-1}. The 550 cm^{-1} and 928 cm^{-1} modes are assigned to ring stretching coupled to a methyl rock and the 615 cm^{-1} and 800 cm^{-1} modes are assigned to symmetric stretches delocalized over the entire cyanine molecule (computational details given in Supporting Information Section 2). The remaining identified modes decay within 1.5 ps after photoexcitation.

Coupling between modes appears as oscillatory features in t_2' due to beating between bright modes or modulations in the Franck-Condon factor of a bright mode by a dark mode. These oscillatory features are distinct from beating due to energetically closely spaced modes as discussed in Supporting Information Section 6.[41,42] A Fourier transform over the t_2' axis generates a correlation plot between ω_2 and ω_2' in which coupling between modes appears as cross peaks. To investigate the oscillatory features observed in Figure 2a, we first decreased the Hann window to 65 fs (Supporting Information Figure 9), thereby isolating higher frequency modulations. We separately Fourier transformed the early time ($t_2' = 0.1 - 1.5$ ps, Figure 2b) and long time ($t_2' = 1.5 - 4.5$ ps, Figure 2c) regions of t_2' to determine the timescale over which mode coupling persists. The early time correlation plot shows a cross peak between 800 cm^{-1} and 315 cm^{-1}, directly reflecting coupling between these modes. The long time correlation plot lacks cross peaks, indicating that the mode coupling decays by 1.5 ps after photoexcitation.

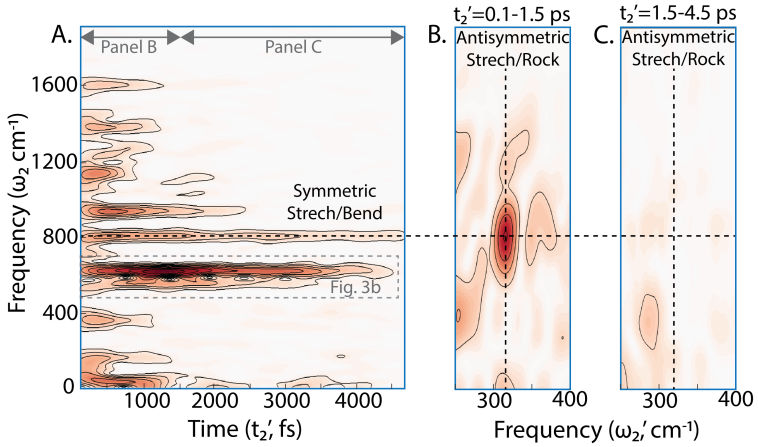

Figure 2: Identification of coupled vibrational modes. (A) Time domain evolution of the power spectrum at an emission frequency of $\omega_3 = 18,620$ cm^{-1} obtained from a 600 fs FWHM sliding Hann window. (B) Coupling between high and low frequency modes based on oscillatory features in 65 fs FWHM sliding window Fourier transform at early times ($0.1 - 1.5$ ps). Frequencies of antisymmetric and symmetric modes shown. (C) Coupling between high and low frequency modes based on oscillatory features in 65 fs FWHM sliding window Fourier transform at late times ($1.5 - 4.5$ ps).

The 800 cm^{-1} mode is a Franck-Condon active symmetric stretch. The 315 cm^{-1} mode is minimally Franck-Condon active. From DFT calculations, we assign the 315 cm^{-1} to

a combination of two antisymmetric stretch modes (301 cm^{-1} and 330 cm^{-1}) localized on the non-nitrogen bound methyl groups. Although the 315 cm^{-1} mode is minimally Franck-Condon active, it modulates the energy and magnitude of the Franck-Condon overlap of the 800 cm^{-1} mode by coupling to this mode. Spectroscopically, this appears as the amplitude modulations of the 800 cm^{-1} mode in the transient grating signal (Supporting Information Figure 9).[41,42]

The phase associated with nuclear wavepackets can be used characterize potential energy surfaces.[43,44] The population subtracted residual transient grating signal is shown as a function of the time delay, t_2, in Figure 3a. The oscillatory features in the residual are primarily due to the symmetric stretch/bend mode at 615 cm^{-1}. The long lifetime and large amplitude of this mode allow it to serve as a reporter mode for the excited state potential energy surface. Two distinct nodes appear at emission frequencies of $\omega_3 = 17,580\ cm^{-1}$ and $\omega_3 = 18,030\ cm^{-1}$, as indicated by dashed lines in Figure 3a. The phase of the 615 cm^{-1} mode is shown in Figure 3a, (top) as a function of emission frequency (ω_3). Two phase jumps appear at the same emission frequencies as the nodes in the oscillatory transient grating signal. A phase jump of π is a well established signature of a potential energy minimum.[43,45] Here, the magnitude of the phase jumps is smaller than π, which occurs when stimulated emission features overlap with the ground state bleach.[46,47]

The two observed jumps correspond to two distinct excited state potential energy minima. The higher frequency phase jump, $\omega_3 = 18,030\ cm^{-1}$, aligns with the peak of the fluorescence emission at $\omega_3 = 17,990\ cm^{-1}$ and therefore corresponds to the bottom of the S_1 potential energy well. This suggests that a large fraction of the 615 cm^{-1} vibrational wavepackets observed at this emission frequency are on the excited state potential energy surface. The magnitudes of the two phase jumps are $0.59 \pm 0.07\ \pi$ and $0.63 \pm 0.07\ \pi$ for the higher and lower frequency jumps, respectively. The similarity of the magnitudes suggests that both phase jumps arise from the same population (same contributions of stimulated emission and ground state bleach signal), which would mean that the lower frequency jump also

comes from the excited state potential energy surface. The lower frequency phase jump, $\omega_3 = 17,580\ cm^{-1}$, corresponds to a non-radiative, dark state, as no peak is observed in this frequency range in either the absorption or emission spectra (Figure 1a, Supporting Information Figure 7a). This state was not previously observed in cyanine dyes. We assign this state to a trans intermediate, as discussed in more detail below. The canonical picture of Cy3 photoisomerization consists of relaxation to the minimum of the S_1 surface, followed by crossing of a thermal barrier to form the TICT state and subsequent isomerization.[29] As the observed state is populated on the ~1 ps timescale, we suggest it serves as an intermediate prior to formation of the TICT state or conversion to the ground state.

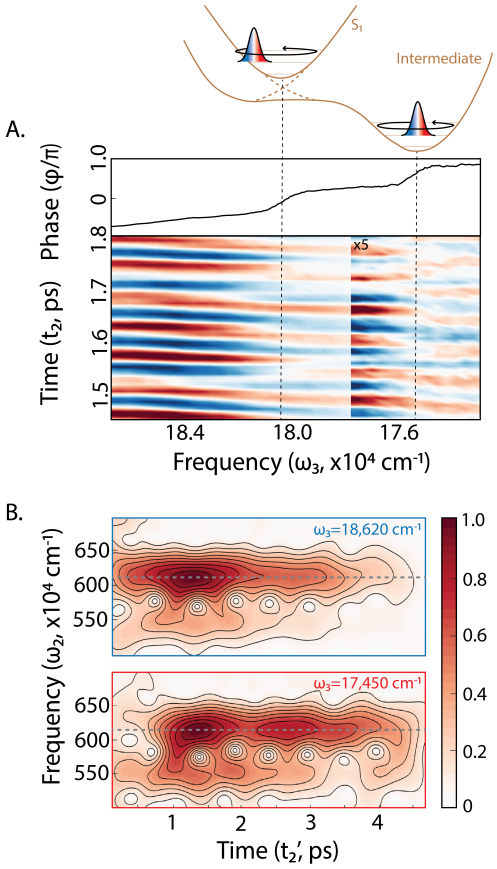

Figure 3: Identification of potential energy surface minima. (A) Time domain transient grating residual as a function of emission frequency. Phase as a function of emission frequency is shown above. Phase jumps are observed at $\omega_3 = 17,580\ cm^{-1}$ and $\omega_3 = 18,030\ cm^{-1}$. (B) Time domain evolution of the power spectrum at an emission frequency of $18,620\ cm^{-1}$ (upper) and $17,450\ cm^{-1}$ (lower) obtained from a 600 fs FWHM sliding Hann window.

To investigate the structural elements that give rise to the observed trans intermediate at $\omega_3 = 17,580\ cm^{-1}$, we investigated the wavepacket dynamics of a Cy3 derivative with a propanol group attached to each nitrogen atom instead of methyl groups (Supporting Information Sections 11 and 12). The propanol-modified Cy3 derivative shows a 110 cm^{-1} redshift in its absorption spectrum. Similarly, we observed a phase jump at $\omega_3 = 17,460$ cm^{-1} for the derivative. Therefore, the non-radiative pathway to the trans intermediate is conserved with a similar energy gap from the S_1 state as in the original Cy3. We also observe mode coupling between a 327 cm^{-1} mode and the 1179 cm^{-1} and 1398 cm^{-1} modes, suggesting vibrational mode coupling occurs on short timescales, similar to the original Cy3. Because propanol and similar modifications are often required intermediates to conjugate Cy3 to a biomolecule of interest, the presence of the trans intermediate in both chromophores establishes the applicability of the result.

Further evidence for the identified trans intermediate state comes from the emission-frequency dependence of the temporal dynamics of the reporter mode, shown for the original Cy3 in Figure 3b. A 600 fs FWHM Hann window was used to generate a sliding window Fourier transform spectrum at regions of high oscillatory signal on the S_1 potential energy surface ($\omega_3 = 18,620\ cm^{-1}$) and on the identified trans intermediate ($\omega_3 = 17,450\ cm^{-1}$). On the S_1 surface, the 615 cm^{-1} mode grows in within $300-400\ fs$. In contrast, on the trans intermediate, the 615 cm^{-1} mode grows in at $1\ ps$ after photoexcitation. The 615 cm^{-1} mode at $\omega_3 = 17,450\ cm^{-1}$ also appears to be $1-2\ ps$ longer-lived than at $\omega_3 = 18,620\ cm^{-1}$. These temporal dynamics could arise due to non-adiabatic relaxation from the higher lying state ($\omega_3 = 18,620\ cm^{-1}$) to the lower lying one ($\omega_3 = 17,450\ cm^{-1}$). The differences in the temporal dynamics also support the conclusion that the two examined emission frequencies correspond to different potential energy surfaces, consistent with the phase jumps in Figure 3a.

The traditional view of photoisomerization of cyanine dyes such as Cy3 and Cy5 is progression along a bond-torsion axis over a thermal barrier into a TICT intermediate (Figure

4a).[33–35,48] Decay from the TICT state is thought to occur through an avoided crossing to the ground state of both the cis and trans isomer. The ground state of the cis isomer undergoes thermal reversion to the ground state of the trans isomer.[49,50] Additional complexity in the excited state manifold and the isomerization pathway has also been suggested. For example, the triplet manifold was proposed to mediate isomerization, but the minimal spin-orbit coupling led to the conclusion that the singlet state dominates on short timescales.[35,51–54] As a result, the photoisomerization pathway shown in Figure 4a has been accepted for several years. Here, we identify an additional state in the excited state potential, a non-radiative trans intermediate state at $\omega_3 = 17,580\ cm^{-1}$, shown in Figure 4b, which is populated on a $\sim 1\ ps$ timescale.

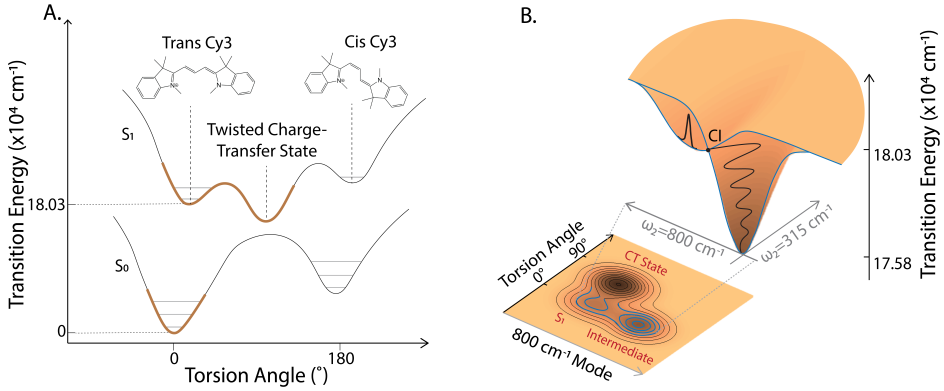

Figure 4: Identification of potential energy surface minima. (A) Potential energy surface for Cy3 isomerization. (B) Potential energy surface for trans intermediate with schematic showing relaxation through a conical intersection mediated by modes at 800 cm^{-1} and 315 cm^{-1}.

We tentatively assign the observed intermediate state to a structural perturbation from the minimum of the radiative S_1 potential.[55] The observed trans intermediate appears on the ∼1 ps timescale, not the hundreds of picoseconds timescale of the TICT state.[35,56] The energy of the intermediate is below the bottom of the S_1 potential (as identified from

the photoluminescence spectrum), which suggests it precedes the TICT or ground state. While we do observe a $\sim$ 45 ps population decay over all emission frequencies consistent with conversion to the TICT,[35,56] the frequency dependent dynamics do not allow us to distinguish between conversion from the S_1 state or the trans intermediate (Supporting Information Figure 6). The observed trans intermediate state is optically dark, and thus it is possible that the trans intermediate state has partial charge-transfer character. However, the extremely small absorption cross-section arising from the symmetry constraints of TICT states makes it unlikely that we would be able to detect such states in our experiment even through the indirect methods employed.[57]

Although the electronic character of the trans intermediate is challenging to determine, our measurements do indicate that it is not a triplet, a cis isomer, nor a $n - \pi^*$ state. First, while the formation of the triplet state has been observed in fluorescence microscopy experiments, the minimal spin-orbit coupling means that intersystem crossing requires much longer than the 1 ps timescale observed.[35,53,54,58,59] Second, photoisomerization to the cis isomer does occur, but it happens on a tens of picoseconds to nanoseconds timescale.[29,35,56] Furthermore, the persistence of the 618 cm^{-1} and 550 cm^{-1} modes at $\omega_3 = 17,580$ cm^{-1}, both of which are highly delocalized over the entire cyanine molecule, excludes large nuclear rearrangement when forming the trans intermediate state. Finally, the insensitivity of the relative energy of the trans intermediate to structural modifications at the indole nitrogen positions also suggests that no large nuclear rearrangement occurs. Third, given the presence of unshared electrons at the nitrogen sites of the cyanine molecule, an $n - \pi^*$ state could be populated through a conical intersection, as has been observed in pyrimidine bases. These states have been calculated to be slightly below the energy of the $\pi - \pi^*$ transition in rhodamine dyes, consistent with our measurements.[60,61] However, these $n-\pi^*$ states are more commonly optically active in azoalkanes, whereas $\pi-\pi^*$ states are more commonly optically active in polyenes, which is particularly true for cyanines.[62] For these reasons, we conclude that the observed trans intermediate state arises upon a minor structural perturbation, such

as a small angle twist.

The observed trans intermediate state is likely populated by a non-adiabatic transition through a conical intersection from the S_1 state, as illustrated in Figure 4b. The minimum model for a conical intersection requires coupling between a symmetric mode corresponding to bond displacement and a non-totally symmetric mode, which breaks symmetry to allow for the intersection of potential energy surfaces.[63–65] Here, we observe coupling between the symmetric 800 cm^{-1} mode and the antisymmetric 315 cm^{-1} mode (non-totally symmetric as shown in Supporting Information Figure 2), consistent with this model. The quantum yield measured in Cy3 (4%) also suggests formation of the trans intermediate state can only be populated for a short time after photoexcitation, consistent with a non-adiabatic transition.[49] The observed trans intermediate is non-radiative and if the ~ 1 ps generation is maintained after photoexcitation, the tens to hundreds of picoseconds radiative relaxation from the S_1 state would be negligible with a quantum yield orders of magnitude lower than the observed value. The mode coupling required for a conical intersection only persists for the first ~ 1.5 ps after photoexcitation. Therefore, the entire population does not have time to transition to the trans intermediate state and the remaining S_1 population undergoes alternative decay pathways, including fluorescence emission.

Structural modifications on the parent fluorophore have been used as a means to enhance fluorescence of cyanine dyes by reducing known non-radiative relaxation pathways.[2,11,12,66–68] For example, Cy3B is a Cy3 analog with a bridging structure that severely restricts photoisomerization and increases the quantum yield from 4% to 67%.[11] Our experiments discovered an additional non-radiative decay pathway, which opens the door to its suppression for further enhancements to the quantum yield. The bridging structure in Cy3B may similarly restrict the non-radiative decay pathway reported here. However, the effect of a bridge cannot be predicted without more complete knowledge of the specific nuclear motion associated with formation of the observed trans intermediate. Alternately, in related small molecule systems, the excitation of specific vibrational modes and collections of vibrational wavepackets

has been shown to control photophysical pathways.[26,69,70] The persistence of mode coupling and the trans intermediate to non-backbone modifications observed here suggests that the C–C stretch modes characteristic to the polyene backbone would be a promising target. A modification to the conjugated backbone of Cy3, such as the addition of a phenyl group (1,1',3,3,3',3'-hexamethyl-9-phenylindocarbocyanine), could disrupt the C-C normal modes along the polyene backbone, thus altering the energetic landscape associated with formation of the trans Cy3 intermediate. Alternately, the 315 cm^{-1} coupled mode implicated in the trans intermediate is largely localized over the methyl group rock/stretching motions, and so modification of this carbon substituent could potentially control mode coupling. An example of this modification from the studied constructs here could be removal of the dimethyl containing carbon, and replacement with either sulfur (3,3'-Dimethylthiacarbocyanine) or oxygen (3,3'-Dimethyloxacarbocyanine), thus disrupting the nuclear motions of the 315 cm^{-1} mode and possibly suppressing formation of the trans intermediate. Either of these nuclear modifications could suppress generation of the identified trans intermediate and thus the newly discovered non-radiative decay pathway to enhance the fluorophore emissive properties.

We used ultrafast transient grating spectroscopy to isolate signatures of nuclear wavepackets that report on the Cy3 excited state potential energy surface and vibrational mode coupling. Our experiments reveal a previously unknown trans intermediate state, likely populated through a conical intersection mediated by coupled modes. The trans intermediate state is optically dark, and so suppression of the state would de-activate a non-radiative decay pathway. Identification of the nuclear motions associated with the coupled modes suggests design principles for molecular analogues with increased fluorescence quantum yields. Optimization of the underlying reaction pathways in molecular dyes provides opportunities to generate fluorophores with superior photophysics for biological imaging and characterization.

Acknowledgement

This work was supported by the U.S Department of Energy Office of Basic Energy Sciences under Award Number DE-SC0019998 (to G.S.S.-C. and M.B.). J.L.B and M.B. also acknowledge support from the Office of Naval Research under Award Numbers N00014-17-1-2609 and N00014-13-1-0664. The high-performance computer cluster used to perform the electronic structure calculations in this work was supported by the Office of Naval Research under Award Number N00014-15-1-2830. S.M.H. acknowledges support from the NSF Graduate Research Fellowship Program. We thank Dr. Jeon Woong Kang and the MIT Laser Biomedical Research Center (LBRC, grant number NIH-5P41EB15871) for assistance with the Raman measurements.

Supporting Information Available

The following files are available free of charge.

- Supporting Information: contains information on general experimental methods, vibrational spectroscopy calculations, characterization of the compressed pulse used in the transient grating experiments, transient grating population dynamics, spectral characterization of Cy3, Fourier analysis of vibration mode coupling, analysis of the emission-frequency dependent growth of the 615 cm^{-1} mode, 615 cm^{-1} and 800 cm^{-1} phase characterization, details of sliding window Fourier analysis, synthesis and spectral characterization on propanol-modified Cy3, and spontaneous Raman anisotropy.
- Cy3-GS.xyz: optimized ground-state structure of Cy3.

References

(1) Wysocki, L. M.; Lavis, L. D. Advances in the Chemistry of Small Molecule Fluorescent Probes. *Current Opinion in Chemical Biology* **2011**, *15*, 752–759.

(2) Lavis, L. D.; Raines, R. T. Bright Ideas for Chemical Biology. *ACS Chemical Biology* **2008**, *3*, 142–155.

(3) Xie, X. S.; Choi, P. J.; Li, G.-W.; Lee, N. K.; Lia, G. Single-molecule Approach to Molecular Biology in Living Bacterial Cells. *Annual Review of Biophysics* **2008**, *37*, 417–444.

(4) Banal, J. L.; White, J. M.; Ghiggino, K. P.; Wong, W. W. Concentrating Aggregation-induced Fluorescence in Planar Waveguides: a Proof-of-Principle. *Scientific Reports* **2014**, *4*, 1–5.

(5) Banal, J. L.; White, J. M.; Lam, T. W.; Blakers, A. W.; Ghiggino, K. P.; Wong, W. W. A Transparent Planar Concentrator Using Aggregates of Gem-Pyrene Ethenes. *Advanced Energy Materials* **2015**, *5*, 1500818.

(6) Uoyama, H.; Goushi, K.; Shizu, K.; Nomura, H.; Adachi, C. Highly Efficient Organic Light-emitting Diodes from Delayed Fluorescence. *Nature* **2012**, *492*, 234–238.

(7) Baldo, M.; Holmes, R.; Forrest, S. Prospects for Electrically Pumped Organic Lasers. *Physical Review B* **2002**, *66*, 035321.

(8) Zheng, Q.; Juette, M. F.; Jockusch, S.; Wasserman, M. R.; Zhou, Z.; Altman, R. B.; Blanchard, S. C. Ultra-stable Organic Fluorophores for Single-molecule Research. *Chemical Society Reviews* **2014**, *43*, 1044–1056.

(9) Zheng, Q.; Lavis, L. D. Development of Photostable Fluorophores for Molecular Imaging. *Current Opinion in Chemical Biology* **2017**, *39*, 32–38.

(10) Dave, R.; Terry, D. S.; Munro, J. B.; Blanchard, S. C. Mitigating Unwanted Photophysical Processes for Improved Single-molecule Fluorescence Imaging. *Biophysical Journal* **2009**, *96*, 2371–2381.

(11) Cooper, M.; Ebner, A.; Briggs, M.; Burrows, M.; Gardner, N.; Richardson, R.; West, R. Cy3B: Improving the Performance of Cyanine Dyes. *Journal of Fluorescence* **2004**, *14*, 145–150.

(12) Michie, M. S.; Götz, R.; Franke, C.; Bowler, M.; Kumari, N.; Magidson, V.; Levitus, M.; Loncarek, J.; Sauer, M.; Schnermann, M. J. Cyanine Conformational Restraint in the Far-red Range. *Journal of the American Chemical Society* **2017**, *139*, 12406–12409.

(13) Chatterjee, S.; Karuso, P.; Boulangé, A.; Peixoto, P. A.; Franck, X.; Datta, A. The Role of Different Structural Motifs in the Ultrafast Dynamics of Second Generation Protein Stains. *The Journal of Physical Chemistry B* **2013**, *117*, 14951–14959.

(14) Paolino, M.; Gueye, M.; Pieri, E.; Manathunga, M.; Fusi, S.; Cappelli, A.; Latterini, L.; Pannacci, D.; Filatov, M.; Leonard, J. Design, Synthesis, and Dynamics of a Green Fluorescent Protein Fluorophore Mimic with an Ultrafast Switching Function. *Journal of the American Chemical Society* **2016**, *138*, 9807–9825.

(15) Son, M.; Pinnola, A.; Bassi, R.; Schlau-Cohen, G. S. The Electronic Structure of Lutein 2 is Optimized for Light Harvesting in Plants. *Chem* **2019**, *5*, 575–584.

(16) Maiuri, M.; Snellenburg, J.; Van Stokkum, I.; Pillai, S.; Wongcarter, K.; Gust, D.; Moore, T. A.; Moore, A. L.; Van Grondelle, R.; Cerullo, G. et al. Ultrafast Energy Transfer and Excited State Coupling in an Artificial Photosynthetic Antenna. *The Journal of Physical Chemistry B* **2013**, *117*, 14183–14190.

(17) Bakulin, A. A.; Rao, A.; Pavelyev, V. G.; van Loosdrecht, P. H.; Pshenichnikov, M. S.; Niedzialek, D.; Cornil, J.; Beljonne, D.; Friend, R. H. The Role of Driving Energy and Delocalized States for Charge Separation in Organic Semiconductors. *Science* **2012**, *335*, 1340–1344.

(18) Musser, A. J.; Liebel, M.; Schnedermann, C.; Wende, T.; Kehoe, T. B.; Rao, A.;

Kukura, P. Evidence for Conical Intersection Dynamics Mediating Ultrafast Singlet Exciton Fission. *Nature Physics* **2015**, *11*, 352.

(19) Nairat, M.; Konar, A.; Kaniecki, M.; Lozovoy, V. V.; Dantus, M. Investigating the Role of Human Serum Albumin Protein Pocket on the Excited State Dynamics of Indocyanine Green using Shaped Femtosecond Laser Pulses. *Physical Chemistry Chemical Physics* **2015**, *17*, 5872–5877.

(20) Caram, J. R.; Fidler, A. F.; Engel, G. S. Excited and Ground State Vibrational Dynamics Revealed by Two–dimensional Electronic Spectroscopy. *The Journal of Chemical Physics* **2012**, *137*, 024507.

(21) Rafiq, S.; Dean, J. C.; Scholes, G. D. Observing Vibrational Wavepackets During an Ultrafast Electron Transfer Reaction. *The Journal of Physical Chemistry A* **2015**, *119*, 11837–11846.

(22) Kudisch, B.; Maiuri, M.; Blas-Ferrando, V. M.; Ortiz, J.; Sastre-Santos, Á.; Scholes, G. D. Solvent-dependent Photo-induced Dynamics in a Non-rigidly Linked Zinc Phthalocyanine–perylenediimide Dyad Probed Using Ultrafast Spectroscopy. *Physical Chemistry Chemical Physics* **2017**, *19*, 21078–21089.

(23) Nairat, M.; Konar, A.; Lozovoy, V. V.; Beck, W. F.; Blanchard, G.; Dantus, M. Controlling S_2 Population in Cyanine Dyes using Shaped Femtosecond Pulses. *The Journal of Physical Chemistry A* **2016**, *120*, 1876–1885.

(24) Schrauben, J. N.; Dillman, K. L.; Beck, W. F.; McCusker, J. K. Vibrational Coherence in the Excited State Dynamics of $Cr(acac)_3$: Probing the Reaction Coordinate for Ultrafast Intersystem Crossing. *Chemical Science* **2010**, *1*, 405–410.

(25) Lee, Y.; Malamakal, R. M.; Chenoweth, D. M.; Anna, J. M. Halogen Bonding Facilitates Intersystem Crossing in Iodo–BODIPY Chromophores. *The Journal of Physical Chemistry Letters* **2020**, *11*, 877–884.

(26) Gueye, M.; Manathunga, M.; Agathangelou, D.; Orozco, Y.; Paolino, M.; Fusi, S.; Haacke, S.; Olivucci, M.; Léonard, J. Engineering the Vibrational Coherence of Vision into a Synthetic Molecular Device. *Nature Communications* **2018**, *9*, 313.

(27) Dean, J. C.; Mirkovic, T.; Toa, Z. S.; Oblinsky, D. G.; Scholes, G. D. Vibronic Enhancement of Algae Light Harvesting. *Chem* **2016**, *1*, 858–872.

(28) Mujumdar, R. B.; Ernst, L. A.; Mujumdar, S. R.; Lewis, C. J.; Waggoner, A. S. Cyanine Dye Labeling Reagents: Sulfoindocyanine Succinimidyl Esters. *Bioconjugate Chemistry* **1993**, *4*, 105–111.

(29) Levitus, M.; Ranjit, S. Cyanine Dyes in Biophysical Research: The Photophysics of Polymethine Fluorescent Dyes in Biomolecular Environments. *Quarterly Reviews of Biophysics* **2011**, *44*, 123–151.

(30) Escobedo, J. O.; Rusin, O.; Lim, S.; Strongin, R. M. NIR Dyes for Bioimaging Applications. *Current Opinion in Chemical Biology* **2010**, *14*, 64–70.

(31) Caselli, M.; Momicchioli, F.; Ponterini, G. Modelling of the cis-trans Partitioning in the Photoisomerizations of Cyanines and Stilbene Derivatives. *Chemical Physics Letters* **1993**, *216*, 41–46.

(32) Dietzek, B.; Brüggemann, B.; Pascher, T.; Yartsev, A. Pump-Shaped Dump Optimal Control Reveals the Nuclear Reaction Pathway of Isomerization of a Photoexcited Cyanine Dye. *Journal of the American Chemical Society* **2007**, *129*, 13014–13021.

(33) Widengren, J.; Schwille, P. Characterization of Photoinduced Isomerization and Back-isomerization of the Cyanine Dye Cy5 by Fluorescence Correlation Spectroscopy. *The Journal of Physical Chemistry A* **2000**, *104*, 6416–6428.

(34) Åkesson, E.; Sundström, V.; Gillbro, T. Solvent-dependent Barrier Heights of Excited-state Photoisomerization Reactions. *Chemical Physics Letters* **1985**, *121*, 513–522.

(35) Stennett, E. M.; Ma, N.; Van Der Vaart, A.; Levitus, M. Photophysical and Dynamical Properties of Doubly Linked Cy3–DNA Constructs. *The Journal of Physical Chemistry B* **2013**, *118*, 152–163.

(36) Dietzek, B.; Yartsev, A.; Tarnovsky, A. N. Watching Ultrafast Barrierless Excited-state Isomerization of Pseudocyanine in Real Time. *The Journal of Physical Chemistry B* **2007**, *111*, 4520–4526.

(37) Ma, F.; Yartsev, A. Ultrafast Photoisomerization of Pinacyanol: Watching an Excited State Reaction Transiting from Barrier to Barrierless Forms. *RSC Advances* **2016**, *6*, 45210–45218.

(38) Mustroph, H.; Reiner, K.; Mistol, J.; Ernst, S.; Keil, D.; Hennig, L. Relationship Between the Molecular Structure of Cyanine Dyes and the Vibrational Fine Structure of their Electronic Absorption Spectra. *ChemPhysChem* **2009**, *10*, 835–840.

(39) Bishop, M. M.; Roscioli, J. D.; Ghosh, S.; Mueller, J. J.; Shepherd, N. C.; Beck, W. F. Vibrationally Coherent Preparation of the Transition State for Photoisomerization of the Cyanine Dye Cy5 in Water. *The Journal of Physical Chemistry B* **2015**, *119*, 6905–6915.

(40) Teramoto, T.; Kobayashi, T. Multiple Mode Coupling in Cy3 Molecules by Impulsive Coherent Vibrational Spectroscopy using a Few-cycle Laser Pulse. *Physical Chemistry Chemical Physics* **2010**, *12*, 13515–13518.

(41) Fuji, T.; Saito, T.; Kobayashi, T. Dynamical Observation of Duschinsky Rotation by Sub-5-fs Real-time Spectroscopy. *Chemical Physics Letters* **2000**, *332*, 324–330.

(42) Kobayashi, T.; Wang, Y.; Wang, Z.; Iwakura, I. Circa Conservation of Vibrational Energy Among Three Strongly Coupled Modes of a Cyanine Dye Molecule Studied by Quantum-beat Spectroscopy with a 7 fs Laser. *Chemical Physics Letters* **2008**, *466*, 50–55.

(43) Cina, J. A.; Kovac, P. A.; Jumper, C. C.; Dean, J. C.; Scholes, G. D. Ultrafast Transient Absorption Revisited: Phase-flips, Spectral Fingers, and Other Dynamical Features. *The Journal of Chemical Physics* **2016**, *144*, 175102.

(44) Ikuta, M.; Yuasa, Y.; Kimura, T.; Matsuda, H.; Kobayashi, T. Phase Analysis of Vibrational Wave Packets in the Ground and Excited States in Polydiacetylene. *Physical Review B* **2004**, *70*, 214301.

(45) Vos, M. H.; Rappaport, F.; Lambry, J.-C.; Breton, J.; Martin, J.-L. Visualization of Coherent Nuclear Motion in a Membrane Protein by Femtosecond Spectroscopy. *Nature* **1993**, *363*, 320.

(46) Du, J.; Teramoto, T.; Nakata, K.; Tokunaga, E.; Kobayashi, T. Real-time Vibrational Dynamics in Chlorophyll a Studied with a Few-cycle Pulse Laser. *Biophysical Journal* **2011**, *101*, 995–1003.

(47) Son, M.; Park, K. H.; Yoon, M.-C.; Kim, P.; Kim, D. Excited-state Vibrational Coherence in Perylene Bisimide Probed by Femtosecond Broadband Pump–probe Spectroscopy. *The Journal of Physical Chemistry A* **2015**, *119*, 6275–6282.

(48) Momicchioli, F.; Baraldi, I.; Berthier, G. Theoretical Study of trans-cis Photoisomerism in Polymethine Cyanines. *Chemical Physics* **1988**, *123*, 103–112.

(49) Chibisov, A.; Zakharova, G.; Görner, H.; Sogulyaev, Y. A.; Mushkalo, I.; Tolmachev, A. Photorelaxation Processes in Covalently Linked Indocarbocyanine and Thiacarbocyanine Dyes. *The Journal of Physical Chemistry* **1995**, *99*, 886–893.

(50) Kuzmin, V.; Darmanyan, A. Study of Sterically Hindered Short-lived Isomers of Polymethine Dyes by Laser Photolysis. *Chemical Physics Letters* **1978**, *54*, 159–163.

(51) Sahyun, M.; Serpone, N. Photophysics of Thiacarbocyanine Dyes: Relaxation Dynamics

in a Homologous Series of Thiacarbocyanines. *The Journal of Physical Chemistry A* **1997**, *101*, 9877–9883.

(52) Köhn, F.; Hofkens, J.; Gronheid, R.; Van der Auweraer, M.; De Schryver, F. C. Parameters Influencing the On and Off Times in the Fluorescence Intensity Traces of Single Cyanine Dye Molecules. *The Journal of Physical Chemistry A* **2002**, *106*, 4808–4814.

(53) Jia, K.; Wan, Y.; Xia, A.; Li, S.; Gong, F.; Yang, G. Characterization of Photoinduced Isomerization and Intersystem Crossing of the Cyanine Dye Cy3. *The Journal of Physical Chemistry A* **2007**, *111*, 1593–1597.

(54) Chibisov, A. Triplet States of Cyanine Dyes and Reactions of Electron Transfer with Their Participation. *Journal of Photochemistry* **1976**, *6*, 199–214.

(55) Improta, R.; Santoro, F. A Theoretical Study on the Factors Influencing Cyanine Photoisomerization: The Case of Thiacyanine in Gas Phase and in Methanol. *Journal of Chemical Theory and Computation* **2005**, *1*, 215–229.

(56) Harvey, B. J.; Levitus, M. Nucleobase-specific enhancement of Cy3 fluorescence. *Journal of fluorescence* **2009**, *19*, 443.

(57) Rettig, W. Charge Separation in Excited States of Decoupled Systems–TICT Compounds and Implications Regarding the Development of New Laser Dyes and the Primary Process of Vision and Photosynthesis. *Angewandte Chemie International Edition in English* **1986**, *25*, 971–988.

(58) Krieg, M.; Redmond, R. W. Photophysical Properties of 3, 3'–dialkylthiacarbocyanine Dyes in Homogeneous Solution. *Photochemistry and Photobiology* **1993**, *57*, 472–479.

(59) Khimenko, V.; Chibisov, A. K.; Görner, H. Effects of Alkyl Substituents in the Polymethine Chain on the Photoprocesses in Thiacarbocyanine Dyes. *The Journal of Physical Chemistry A* **1997**, *101*, 7304–7310.

(60) Hare, P. M.; Crespo-Hernández, C. E.; Kohler, B. Internal Conversion to the Electronic Ground State Occurs via Two Distinct Pathways for Pyrimidine Bases in Aqueous Solution. *Proceedings of the National Academy of Sciences* **2007**, *104*, 435–440.

(61) Moore, B.; Schrader, R. L.; Kowalski, K.; Autschbach, J. Electronic π-to-π^* Excitations of Rhodamine Dyes Exhibit a Time-Dependent Kohn–Sham Theory "Cyanine Problem". *ChemistryOpen* **2017**, *6*, 385–392.

(62) Sanchez-Galvez, A.; Hunt, P.; Robb, M. A.; Olivucci, M.; Vreven, T.; Schlegel, H. B. Ultrafast Radiationless Deactivation of Organic Dyes: Evidence for a Two-state Two-mode Pathway in Polymethine Cyanines. *Journal of the American Chemical Society* **2000**, *122*, 2911–2924.

(63) Heider, N.; Fischer, S. F. Multimode Effects in Molecular Spectra Involving Vibronically Coupled Excited States with Application to Pyrazine. *Chemical Physics* **1984**, *88*, 209–220.

(64) Domcke, W.; Köppel, H.; Cederbaum, L. Spectroscopic Effects of Conical Intersections of Molecular Potential Energy Surfaces. *Molecular Physics* **1981**, *43*, 851–875.

(65) Hoffman, D. P.; Ellis, S. R.; Mathies, R. A. Characterization of a Conical Intersection in a Charge-transfer Dimer with Two-dimensional Time-resolved Stimulated Raman Spectroscopy. *The Journal of Physical Chemistry A* **2014**, *118*, 4955–4965.

(66) Grimm, J. B.; English, B. P.; Chen, J.; Slaughter, J. P.; Zhang, Z.; Revyakin, A.; Patel, R.; Macklin, J. J.; Normanno, D.; Singer, R. H. et al. A General Method to Improve Fluorophores for Live-cell and Single-molecule Microscopy. *Nature Methods* **2015**, *12*, 244.

(67) Grimm, J. B.; Muthusamy, A. K.; Liang, Y.; Brown, T. A.; Lemon, W. C.; Patel, R.; Lu, R.; Macklin, J. J.; Keller, P. J.; Ji, N. et al. A General Method to Fine-tune Fluorophores for Live-cell and in vivo Imaging. *Nature Methods* **2017**, *14*, 987.

(68) Hall, L. M.; Gerowska, M.; Brown, T. A Highly Fluorescent DNA Toolkit: Synthesis and Properties of Oligonucleotides Containing New Cy3, Cy5 and Cy3B Monomers. *Nucleic Acids Research* **2012**, *40*, e108–e108.

(69) Stensitzki, T.; Yang, Y.; Kozich, V.; Ahmed, A. A.; Kössl, F.; Kühn, O.; Heyne, K. Acceleration of a Ground-state Reaction by Selective Femtosecond-infrared-laser-pulse Excitation. *Nature Chemistry* **2018**, *10*, 126.

(70) Nenov, A.; Borrego-Varillas, R.; Oriana, A.; Ganzer, L.; Segatta, F.; Conti, I.; Segarra-Marti, J.; Omachi, J.; Dapor, M.; Taioli, S. et al. UV-light-induced Vibrational Coherences: The Key to Understand Kasha Rule Violation in Trans-azobenzene. *The Journal of Physical Chemistry Letters* **2018**, *9*, 1534–1541.